ACADEMIA ROMÂNĂ
Revue Roumaine de Chimie
http://web.icf.ro/rrch/

Rev. Roum. Chim.,
2017, *62*(6-7), 539-544

PHASE RELATIONS IN THE NiTiCu SHAPE MEMORY MATERIALS USED IN MEDICINE APPLICATIONS

Cristiana Diana CIRSTEA,[a*] Marcela MIHAI,[b] Vasile CIRSTEA[c], Delia PATROI,[a] Haritina CHIVU,[d] Florina RADULESCU,[a] Violeta TSAKIRIS,[a] Otilia CULICOV[a,e] and Anatol Mihail BALAGUROV[e]

[a] National Institute for Research and Development in Electrical Engineering INCDIE ICPE-CA, Splaiul Unirii, nr. 313, Sector 3, 030138, Bucharest, Roumania
[b] "Petru Poni" Institute of Macromolecular Chemistry of Roumanian Academy, 41A Grigore Ghica Voda Alley, 700487 Iasi, Roumania
[c] Military Equipments and Technologies Research Agency, Strada Aeroportului, nr. 16, Clinceni, 077025, Ilfov, Roumania
[d]School, no.5, 114 Victoria Alley, Sector 1, 10092 Bucharest, Roumania
[e]Joint Institute for Nuclear Research Frank Laboratory of Neutron Physics, Joliot-Curie 6, Dubna, 141980, Moscow region, Russia

Received November 2, 2016

The paper studies the effect of copper added in an amount of up to 10 at.% on the structure and phase transformation in ternary $Ni_{50-x}Ti_{50}Cu_x$ materials, $0 \leq Cu \leq 10\%$, obtained by spark plasma sintering with and without mechanical alloying. These effects have been investigated by X-ray diffraction, scanning electronic microscopy together with energy dispersive X-ray spectroscopy and nanoindentation measurements. Also the quality of the materials was characterized by porosity and density.

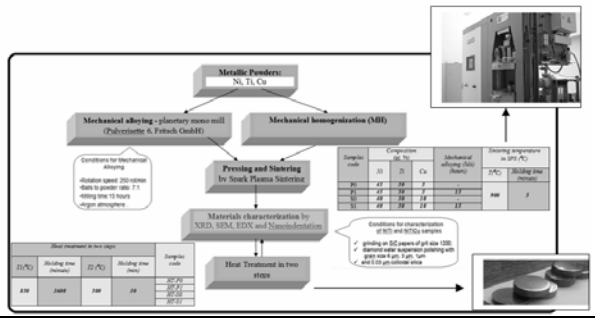

INTRODUCTION

Shape memory materials (SMMs) are the materials that have the property of remembering their original shape based on dual-phase transition transformation (austenite and martensite phases) under certain conditions of temperature and pressure. This phase transition occurs without diffusion and it is called martensitic transformation. The dual-phase microstructure of shape memory alloys consists of the austenite phase, stable in high energy levels with a cubic (B2) structure, and the martensite phase with monoclinic (B19') or orthorhombic (B19) structures.[1-7]

SMMs have shape memory effect and pseudoelasticity properties, which have made them attractive candidates for many applications in different fields of engineering and science.[1] Also, due to this unique combination of mechanical properties, SMMs possess great promise as biomaterials for medicine application.[2-6]

It is well known that the shape memory properties of the shape memory alloys (NiTi) depend on the addition of a third element like copper, iron or niobium, these having a major influence on the martensitic transformation temperature. Thus, adding Cu reduces the range of transformation temperature and increases the strength difference between the austenite and martensite phases. Also, the addition of Cu to $Ni_{50}Ti_{50}$ can stabilize the additional B19-phase, associated with a two step transformation from B2 to B19' by B19 phase.[8] When the Cu percentage is less than 5 at.%, the transformation is the same as in the binary NiTi system, *i.e.*, (B2)↔(B19'),

* Corresponding author: diana.cristea@icpe-ca.ro

compared with the range of 5 to 8 at.% Cu, where a two-step martensitic transformation occurs, *i.e.*, (B2)→(B19) and then (B19)→(B19'). In case of Cu percentage between 10 and 20 at.%, it leads only to (B2)↔(B19) transformation, which is accompanied by a reduction of the elastic modulus.[4,5] Some studies showed that materials like NiTiCu improve the corrosion resistance.[9-11]

From the point of view of processing shape memory materials by powder metallurgy[12,13] was shown that, because of mechanical alloying process, a great amount of vacancies, dislocations and associated lattice strain were introduced into NiTi. The NiTi powders obtained by mechanical alloying presented an amorphous structure, when both martensite and austenite phase can coexist. The heat treatments are effective methods to improve mechanical and shape memory properties of Ni-rich alloys. This is mostly due to the formation of coherent Ni_4Ti_3 precipitates which cause coherency stress fields in the microstructure influencing martensitic transformation characteristics, increasing transformation temperatures by depleting Ni-content of the matrix, and increasing critical stress for slip.[6,7] When Cu is added in the composition of the NiTi shape memory materials can appear precipitates like $(Ni,Cu)Ti_2$ or Ni_2Ti.[14-16]

The paper presents the result of investigations of phase transformation and the effect of copper added in an amount of up to 10 at.% in the structure of ternary $Ni_{50-x}Ti_{50}Cu_x$ materials ($0 \leq Cu \leq 10\%$) obtained by unconventional technologies like spark plasma sintering (SPS) with and without mechanical alloying. The NiTiCu materials were investigated using X-ray diffraction (XRD), scanning electronic microscopy together with energy dispersive X-ray spectroscopy (SEM/EDX) and nanoindentation measurements. The quality of these materials, as concern porosity and density, was characterized too.

RESULTS AND DISCUSSION

The characterization of crystalline microstructure of NiTiCu samples contributes to the control of the manufacturing process by SPS. In order to estimate the relative amount of each crystalline phase, the XRD experimental spectrum was simulated using the Rietveld method by Maud software. The technique of X-ray diffraction is still considered the most suitable for quantitative analysis of phases.[17] Values of reliability factors, which prove goodness of the refinement, were below 7%. The results from simulated XRD patterns of the investigations applied to NiTiCu samples obtained by SPS at 900^0C without mechanical alloying (P0) and with 15 hours mechanical alloying (P1 and S1) are presented in Figure 1 and Table 1, as compared to the results obtained for NiTiCu samples after heat treatment (HT-P0, HT-P1, HT-S0, HT-S1) applied in two steps at 850^0C and 500^0C in argon atmosphere.

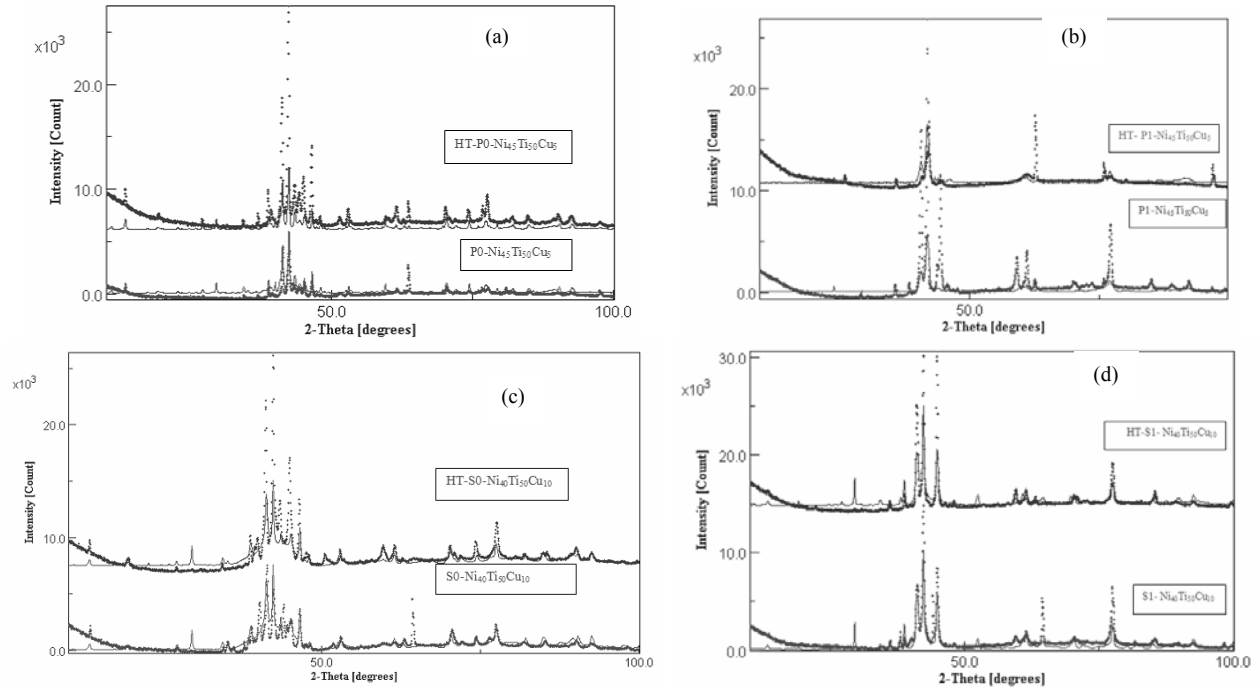

Fig. 1 – Simulated XRD results of NiTiCu sample processed by SPS at 900ºC, before and after the two steps heat treatment (HT) for (a) P0 and HT-P0; (b) P1 and HT-P1; (c) S0 and HT-S0; (d) S1 and HT-S1.

Analysis of the diffraction pattern of the NiTiCu alloy revealed the presence of B2, B19 and/or B19' phases and typical precipitates like Ni_3Ti, Ni_2Ti, $NiTi_2$, and $Ti_2(Ni,Cu)$. The structural data of the observed phases are shown in Table 1. Two things can be noticed after applying the HT: the phase amount calculated by refinement (Rietveld method) for the identified precipitates was reduced (see Table 1) and the amount of martensite phase was increased. Application of mechanical alloying up to 15 hours in the process of making samples led to decreasing the percentage of martensite phase identified in NiTiCu samples (P0 and S0) and led to increasing of Ni_2Ti precipitates. Also, in the 5% Cu (P0) ternary alloy without mechanical alloying were identified the three phases characteristic to martensitic transformation. These identified phases confirmed that the martensitic transformation will be accomplished through a two-step transformation B2↔B19↔B19', the result being consistent with that obtained by some authors[4,7,18,19] for a NiTiCu alloy with 10% at. Cu.

In the P1 samples (5%at. Cu ternary alloy) with mechanical alloying was also identified the R phase, which usually occurs in NiTi alloys with concentrations of Ni between 50.8 and 51 at.%.[20,21] In the other samples the possible martensitic transformation is B2↔B19'. The formation of these phases in NiTiCu alloys is reported by some papers[15,16,20] but also by SEM / EDX measurements.

The SEM / EDX analyses can be used to calculate the ratio of the alloying elements and the results are presented in Table 2. In case of P0 and P1 samples, the results are consistent with the literature.[21-24] From the microstructural point of view, we believe that, after applying the heat treatment, the structure was the same (heterogeneous) which suggests that there has been a recrystallization reaction. This structure was also obtained by M. Ghadiri *et al.*[24] for NiTiCu obtained by vacuum induction melting method with nominal composition of $Ti_{50.4}Ni_{49.6-x}Cu_x$ (x = 0, 3, 5, 7 at.%). Some areas corresponding to the undissolved Ni phase where identified by EDX (P0 sample) and also some precipitate phases like Ni_3Ti_2 (especially for samples that have been applied the heat treatment: HT-P0, HT-P1 and HT-S1), $Ni_2(Ti,Cu)$ (for HT-P1 and HT-S1 samples) or $(Ni,Ti)_2Cu$ (for P1 sample). These phases do not appear in XRD analysis because the amount of phase in material is too small to be detected. In the case of samples without mechanical alloying (P0 and S0), is observed that in their microstructure is a structure of irregularly shaped grains. In this structure, small particles are formed around the large ones creating something like a cluster. In some studies[15], the occurrence of $NiTi_2$ precipitation is associated with the reaction of Cu with Ni and Ti atoms, but also with the increasing of the material hardness, as shown in Table 3. The Ni_3Ti minority phase identified from the Rietveld analysis usually occurs at 900^0C, and after the heat treatment this phase fraction decrease, except S1 sample where the phase fraction of Ni_3Ti precipitate was not identified. The results of X-ray diffraction of the NiTiCu samples have verified the results of the SEM analysis.

The calculation of the porosity of these materials was conducted by Archimedes method[24] and the results are shown in the table 3. Even if the structure is inhomogeneous, because of the presence of precipitate phases that were identified, the NiTiCu materials density is higher when copper content increases from 5 to 10 at.%, while porosity is less than 5%. Exception makes the P1 sample where porosity was 10%. After applying the HT, the density decreased for HT-P0 and HT-P1, which led to increased porosity. In case of HT-S0 and HT-S1, the applied HT led to increased density that is in agreement with the value reported by Y.Du et al.[23].

Table 1

Relative percentage of the crystalline phases calculated by Rietveld method for NiTiCu materials

Phase (%wt)	NiTi cubic (B2)	NiTi monoclinic (B19')	NiTiCu (B19)	$NiTi_2$	$(CuNi)Ti_2$	Ni_2Ti	R-phase	Ni_3Ti
P0	3.47±0.41	25.93±4.94	6.29±0.48	51.78±4.15	6.95±1.25	1.23±1.02	-	4.32±0.51
HT-P0	2.73±0.56	37.70±0.68	4.85±0.68	39.08±4.17	4.82±1.95	6.44±3.90	-	4.36±0.80
P1	-	3.02±0.30	19.62±1.34	3.61±1.83	-	65.80±1.57	3.50±0.14	4.41±1.94
HT-P1	-	3.72±0.08	14.21±0.77	1.89±1.79	-	74.08±1.06	2.84±0.60	3.23±1.10
S0	2.35±0.30	59.66±6.12	-	34.98±3.91	-	-	-	3.32±0.40
HT-S0	1.85±0.10	75.50±3.81	-	20.43±1.32	-	-	-	2.20±0.15
S1	3.66±0.26	19.41±0.0	-	20.67±2.1	-	56.24±5.28	-	-
HT-S1	3.79±0.28	22.84±0.0	-	19.81±2.08	-	53.54±6.33	-	-

Table 2

Results of SEM and EDX measurements

P0-$Ni_{45}Ti_{50}Cu_5$, without mechanical alloying

Spectrum	Ti(%wt)	Ni(%wt)	Cu(%wt)	Phase
Spectrum 1	11.54	86.41	2.04	Ni
Spectrum 2	46.05	45.41	8.53	NiTiCu
Spectrum 3	62.38	33.30	4.32	Ti_2(Ni,Cu)
Spectrum 4	45.03	51.84	3.14	NiTi
Spectrum 5	15.44	83.91	0.65	Ni
Spectrum 6	59.02	37.22	3.76	Ti_2(Ni,Cu)
Std. deviation	2.62	2.24	2.69	

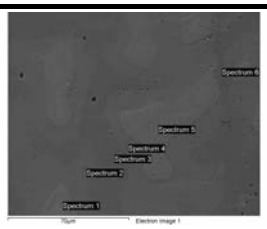

HT - P0 - $Ni_{45}Ti_{50}Cu_5$, without mechanical alloying

Spectrum 1	46.01	47.81	6.17	NiTiCu
Spectrum 2	61.75	33.55	4.69	$NiTi_2$
Spectrum 3	45.94	42.46	11.61	Ni_3Ti_2
Spectrum 4	61.29	33.44	5.27	$NiTi_2$
Spectrum 5	53.26	40.46	6.29	Ti_2(Ni,Cu)
Std. deviation	7.84	6.2	2.56	

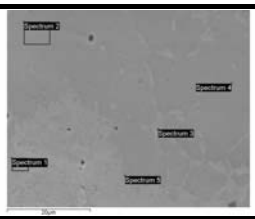

P1 - $Ni_{45}Ti_{50}Cu_5$, with 15h mechanical alloying

Spectrum 1	47.94	49.26	2.80	NiTi
Spectrum 2	43.29	49.33	7.38	NiTiCu
Spectrum 3	47.89	49.57	2.54	NiTi
Spectrum 4	36.18	49.11	14.71	$(Ni,Ti)_2Cu$
Spectrum 5	46.22	48.69	5.09	NiTiCu
Spectrum 6	49.25	47.54	3.21	$(Ni,Cu)Ti_2$
Std. deviation	4.84	0.73	4.66	

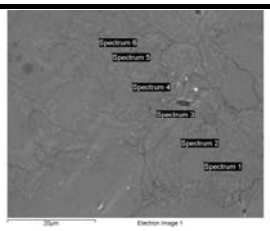

HT - P1 - $Ni_{45}Ti_{50}Cu_5$, with 15h mechanical alloying

Spectrum 1	24.32	65.98	5.85	Ni_2Ti
Spectrum 2	45.67	46.34	4.46	NiTi
Spectrum 3	27.26	53.74	12.41	Ni_3Ti_2
Spectrum 4	29.1	54.06	11.06	Ni_2(Ti,Cu)
Spectrum 5	29.46	53.32	12.07	Ni_2(Ti,Cu)
Spectrum 6	34.4	50.63	9.97	NiTiCu
Spectrum 7	33.72	48.94	9.22	NiTiCu
Spectrum 8	24.28	66.07	4.58	Ni_2Ti
Std. deviation	3.93	2.07	5.18	

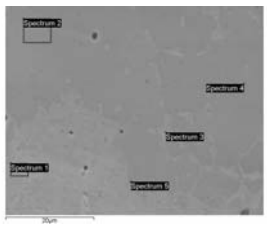

S0 - $Ni_{40}Ti_{50}Cu_{10}$, without mechanical alloying

Spectrum 1	62.20	33.49	4.31	$NiTi_2$
Spectrum 2	62.81	32.58	4.61	$NiTi_2$
Spectrum 3	45.08	48.79	6.13	NiTi
Spectrum 4	46.74	45.95	7.32	NiTi
Spectrum 5	62.25	33.02	4.73	$NiTi_2$
Spectrum 6	60.97	34.60	4.43	$NiTi_2$
Std. deviation	8.38	7.29	1.21	

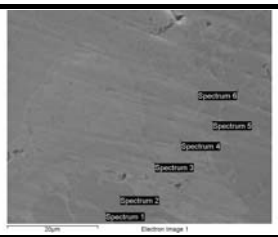

HT - S0 - $Ni_{40}Ti_{50}Cu_{10}$, without mechanical alloying

Spectrum 1	60.19	34.31	5.51	$NiTi_2$
Spectrum 2	42.45	48.45	9.10	NiTi
Spectrum 3	30.86	39.37	29.77	NiTiCu
Std. deviation	2.40	5.88	1.26	

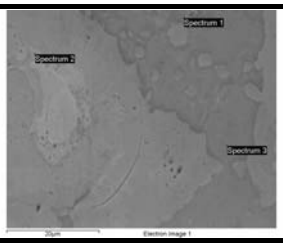

Table 2 (continued)

S1 - $Ni_{40}Ti_{50}Cu_{10}$, with 15h mechanical alloying					
Spectrum 1	42.92	41.45	15.63	NiTi	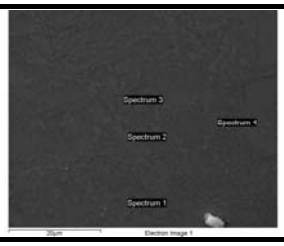
Spectrum 2	46.82	44.04	9.14	NiTi	
Spectrum 3	48.33	37.69	13.97	$(Ni,Cu)Ti_2$	
Spectrum 4	44.38	44.97	10.65	NiTi	
Std. deviation	2.43	3.26	2.98		
HT - S1 - $Ni_{40}Ti_{50}Cu_{10}$, with 15h mechanical alloying					
Spectrum 1	46.90	46.60	6.51	NiTi	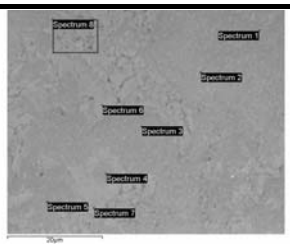
Spectrum 2	43.61	45.08	11.30	$NiTi_2$	
Spectrum 3	45.30	49.09	5.61	NiTi	
Spectrum 4	49.51	44.66	5.84	Ni_3Ti_2	
Spectrum 5	47.87	46.17	5.96	Ni_3Ti_2	
Spectrum 6	31.57	44.63	23.79	$Ni_2(Ti,Cu)$	
Spectrum 7	39.59	45.26	15.14	NiTi	
Spectrum 8	39.68	46.02	14.29	NiTi	
Std. deviation	5.79	1.52	6.54		

Table 3

Results of nanoindentation, density and porosity measurements

	Type of sample	**Vickers hardness (HV)**	**E (GPa)**	**Density (g/cm3)**	**Porosity (%)**
Before and after heat treatment	P0=$Ni_{45}Ti_{50}Cu_5$ without mechanical alloying	328±21.85	79±1.39	6.319	1.866
	HT-P0=$Ni_{45}Ti_{50}Cu_5$ without mechanical alloying	396±15.23	71±12.30	5.663	9.19
Before and after heat treatment	P1=NiTiCu with mechanical alloying	266±14.40	84±3.45	5.55	10.529
	HT-P1=$Ni_{45}Ti_{50}Cu_5$ with mechanical alloying	646±0.50	82±8.89	5.041	18.735
Before and after heat treatment	S0=$Ni_{40}Ti_{50}Cu_{10}$ without mechanical alloying	803±17.40	95±4.97	6.518	4.934
	HT-S0=$Ni_{40}Ti_{50}Cu_{10}$ without mechanical alloying	326±32.17	70±15.4	6.664	3.286
Before and after heat treatment	S1=$Ni_{40}Ti_{50}Cu_{10}$ with mechanical alloying	659±31.11	97±3.83	5.984	3.58
	HT-S1=$Ni_{40}Ti_{50}Cu_{10}$ with mechanical alloying	545±47.82	94±8.54	6.318	2.716

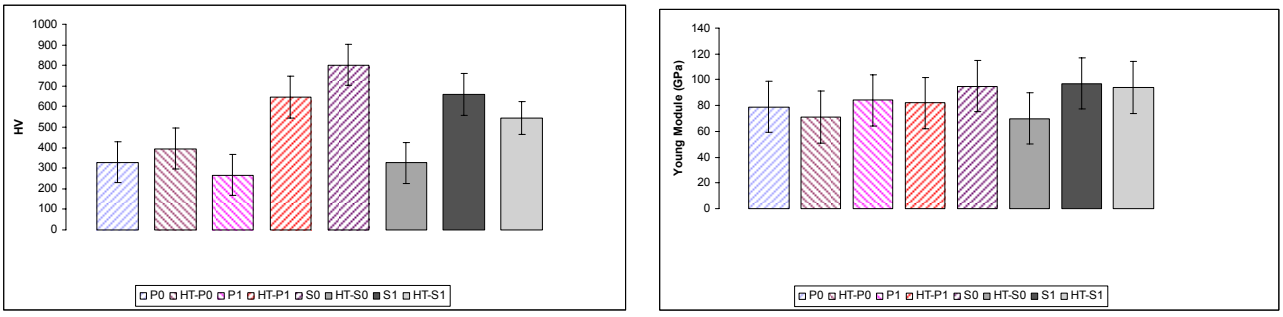

Fig. 2 – Results of Vickers hardness and Young module for NiTiCu samples.

These measurements allowed a direct correlation of the microstructure evolution with the secondary hardening phenomenon (observed by nanoindentation measurements), namely the hardness HV that is decreased for all the samples with mechanical alloying (P1 and S1) comparative with the samples without mechanical alloying (P0 and S0) before HT, the data being correlated to the literature[9-11]. After applying the heat treatment, it can be noticed that HV increases for HT-P0 and HT-P1, and decreases for HT-S0 and HT-S1 due to the variety of the identified precipitates (Figure 2). The Young modulus value classifies the materials achieved by SPS combined or not with MA as austenitic type according to literature[12].

EXPERIMENTAL

The samples used in this study were made from elemental powder by spark plasma sintering method without (P0 and S0) and with mechanical alloying up to 15 hours (P1 and S1). The nominal composition was $Ni_{45}Ti_{50}Cu_5$ (P0) and $Ni_{40}Ti_{50}Cu_{10}$

(S0). The cylindrical samples with diameter of 20 mm and height of 4-5 mm were realized in vacuum by uniaxial pressing with 50 MPa at a sintering temperature of 900 ºC and holding time of 5 minutes. In order to increase the alloy homogeneity, the NiTiCu samples were subjected to a heat treatment (HT) in two steps as follows: temperature increasing with 100ºC/min until 850ºC, holding for 1 hour, cooling with 100ºC/min until 500ºC, holding for 30 min and cooling again at room temperature with 100ºC/min in argon atmosphere. After heat treatment the samples are noted with HT-P0, HT-P1, HT-S0 and HT-S1. Due to the easy oxidation of Ti, the samples were made in vacuum (for SPS) and argon for heat treatment. Thus, the material that was observed microscopically, was also analyzed by XRD and SEM/EDX measurements. The diffraction data were obtained at room temperature using a Bruker diffractometer with Cu X-ray tube anode, λ=1.5406Å, Göbell mirror, 1D Lynx Eye detector. The measurements were performed with an increment angle $2\theta = 0.04^0$, with a scan speed of 1 s/step. Qualitative identification was done using ICDD database PDF2 Release 2014 records associating the corresponding theoretical to the main crystallographic phases. The Rietveld method was used to calculate phase fraction of the most important phases of NiTiCu samples. In order to identify the correct phase, it was necessary to fit the peak profile with each one of these phases and, after this, refinements were done with each phase. SEM and EDX analyses were performed using a scanning electron microscope (Auriga, Carl Zeiss SMT) and were used to study the composition of phases. The density determination is performed by means of Archimedes' principle with Metter Toledo apparatus. To determine the density, measurements were performed using alcohol. The porosity was calculated with mathematic formula presented by T. Goryczka et al.[21,22]. The theoretical density for NiTiCu was 6.21g/cm^3 with 10%atCu and 6.20g/cm^3 for NiTiCu with 5%atCu in composition in this study. The conditions of applying mechanical alloying and nanoindentation measurements are described by C. D. Cirstea *et al.*[18]

CONCLUSIONS

This paper extends the state of knowledge about the technological possibilities of the NiTiCu shape memory alloy manufacturing. In summary, the combined use of XRD and SEM/EDX allows to obtain a detailed description of NiTiCu microstructure. The majority phase identified by XRD and EDX was B19', corresponding to monoclinic martensite phase and precipitate phases. Application of mechanical alloying up to 15 hours in the process of making samples led to increasing the percentage of martensite phase identified in NiTiCu samples. The nanoindentation measurements allowed a direct correlation of the microstructure evolution with the secondary hardening phenomenon due to precipitate phases. The Young modulus value classifies the materials achieved by SPS combined or not with MA as austenitic.

Acknowledgement: This research was supported by the Bilateral Collaboration Roumania – JINR under the Project No. 62/2016 (JINR Orders 95 and 96/15.02.2016).

REFERENCES

1. S. Sadat, J. Salichs, M. Nori, Z. Hou, H. Davodi, I. Baron, Y. Suzuki and A. Masuda, *Smart Mater. Struct*., **2002**, *11*, 218–229.
2. S.M. Seyyed Aghamiri, M. Nili Ahmadabadi, H. Shahmir, F. Naghdi, Sh. Raygan, *J. Mechan. Behavior Biomed. Mater.*, **2013**, *21*, 32–36
3. S.M. Seyyed Aghamiri, M. Nili Ahmadabadi, Sh. Raygan, *J. Mechan. Behavior Biomed. Mater.*, **2011**, *4*, 298–302
4. S. Barbarino, E. I. Saavedra Flores, R. M. Ajaj, I. Dayyani and M. I. Friswell, *Smart Mater. Struct*., **2014**, *23*, 063001.
5. J. van Humbeeck, *J. Phys. IV France,* **1997**, *7*, C5-3 – C5-12.
6. D. J. Fernandes, R. V. Peres, A. M. Mendes and C. N. Elias, *ISRN Dent*., **2011**, *2011*, 132408 -1324014
7. T.W. Duering and A.R. Pelton, "Materials properties Handbook: Titanium Alloys, Ti-Ni Shape memory alloys", ASM International, 1994.
8. E. Povoden-Karadeniz, D.C. Cirstea and E. Kozeschnik, *Mater. Sci. Eng*. **2016**, *123*, 12038-12044.
9. B. O'Brien and M. Bruzzi, "Comprehensive Biomaterials", Elsevier, Oxford, 2011, p. 49-72
10. F. J. Gil and J. A. Planell, *J. Biomed. Mater. Res*., **1999**, *48*, 682-688.
11. M. J. Yaszemski, "Biomaterials in Orthopedics Handbook", Taylor & Francis Group, New York, 2003.
12. F. Neves, I. Martins, J. B. Correia, M. Oliveira and E. Gaffet, *Intermetallics*, **2007**, *15*, 1623−1631.
13. K. Saitoh, K. Kubota and T. Sato, *Technische Mechanik*, **2010**, *30*, 269 – 279.
14. W.J. Moberly, J . L. Proft, T.W. Duerig and R. Sinclair, *Mater. Sci. Forum*, **1990**, *56 – 58*, 605-610.
15. M. Morakabati, Sh. Kheirandish, M. Aboutalebi, A. Karimi Taheri and S. M. Abbasi, *J. Alloys Compounds*, **2010**, *499*, 57-62.
16. T. H. Nam, T. Saburi, Y. Nakata and K. Shimizu, *Materials Transactions*, **1990**, *31*, 1050-1056.
17. C. T. Kniess, J. Cardoso de Lima and P. B. Prates, "Sintering - Methods and Products" Intech, Rijeka, 2012, p. 293-316, http://cdn.intechopen.com/pdfs/33188, http://goo.gl/NWoIs4.
18. C. D. Cirstea, M. Lungu, A. M. Balagurov, V. Marinescu, O. Culicov, G. Sbarcea and V. Cirstea, *Adv. Eng. Forum*, **2015**, *13*, 83-90.
19. T. Fukuda, T. Saburi, T. Chihara and Y. Tsuziki, *Materials Transactions*, **1995**, *36*, 1244-1248.
20. M. Nishida and C.M. Wayman, *Metallurgical Transactions A*, **1986**, *17*, 1505-1515.
21. T. Goryczka and J. Van Humbeeck, *J. Achiev. Mater. Manufact. Eng.,* **2006**, *17*, 65-68.
22. T. Goryczka, **2013** (http://creativecommons.org/licenses/by/3.0)
23. Y. Du and J. C. Schuster, *Z. Metallkd*., **1998**, *89*, 399–410.
24. M. Ghadiri and A. Saidi, *J. Adv. Mater. Proces*., **2014**, *2*, 47-54.